WAVELET ANALYSIS OF THE TIMING OF INDIVIDUAL COMPONENTS OF THE ECG SIGNAL

Burke, M. J. Nasor, M.

Dept. of Electronic and Electrical Engineering, Trinity College, Dublin 2, Rep. of Ireland.

ABSTRACT

ECG recordings were obtained from 21 healthy subjects aged between 13 and 65 years, over a range of heart rate extending from 46 to 184 beats/min (bpm). A wavelet transform method, based on the Mexican Hat wavelet was then used to precisely locate the positions of the onset, peak and termination of individual components in the ECG signal. These times were then classified according to the heart rate associated with the cardiac cycle to which the component belonged. Second order equations in the square root of the cardiac cycle time, T_{R-R} of the form $A.\sqrt{T_{R-R}} + B.T_{R-R} + C$ were fitted to the data obtained for each component to characterize its timing variation.

1. INTRODUCTION

The components of the electrocardiogram are defined in Fig.1. It is broadly recognized that the durations of individual components vary with heart rate in a non-linear manner. The earliest attempt to quantify this relationship was made by Bazett [1] and his results are still cited in many instances where no other information is available. Bazett formulated equations characterizing the duration of three of the ECG components as a function of the cardiac cycle time as follows:

$$\text{Q}-\text{T Interval} \qquad T_{Q-T} = 0.37\sqrt{T_{R-R}} \quad \text{s} \qquad (1)$$

$$\text{P}-\text{R Interval} \qquad T_{P-R} = 0.06 - 0.10\sqrt{T_{R-R}} \quad \text{s} \qquad (2)$$

$$\text{QRS Complex} \qquad T_{QRS} = 0.03 - 0.04\sqrt{T_{R-R}} \quad \text{s} \qquad (3)$$

where T_{R-R} is the cardiac cycle time measured between peaks of successive QRS complexes or R-waves. Later researchers, including the authors, have questioned the accuracy of Bazett's formulae, with most comment being concerned with the Q-T interval because of its clinical importance [2,3]. Much work has been done on providing reliable means of detecting the QRS complexes in the ECG, primarily for triggering purposes, but no comprehensive study examining the variation in the timing of the individual components as a function of heart rate has been carried out. This article reports such a study.

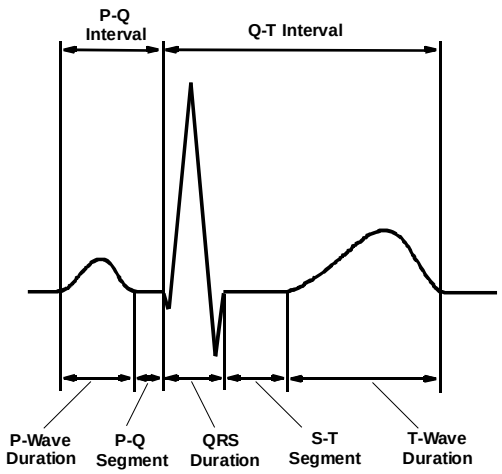

Fig. 1 A typical ECG signal profile with timing of components defined

2. WAVELET ANALYSIS

In order to locate individual waves in the ECG signal accurately, a wavelet having a similar profile is required and the Mexican Hat wavelet shown in Fig. 2 makes an ideal choice in this regard. The basic Mexican Hat wavelet is described in the continuous time domain as:

$$\psi(t) = \frac{2}{\sqrt{3}}\pi^{-\frac{1}{4}}(1-t^2)e^{-t^2/2} \qquad (4)$$

A family of analyzing wavelets in the time-frequency domain is obtained by applying a scaling factor a and a translation factor τ to the basic mother wavelet defined by eqn.4 to give:

$$\psi_{a,\tau} = \frac{1}{\sqrt{a}}\psi\left(\frac{t-\tau}{a}\right) \qquad (5)$$

2.1. Wavelet Transform

When applied to a continuous-time signal $s(t)$ the Wavelet Transform is defined as:

$$W_{\psi,s}(a,\tau) = \int_{-\infty}^{+\infty} s(t)\psi_{a,\tau}(t)dt \qquad (6)$$

where a value of the transform is obtained for chosen values of a and τ. The transform is calculated at discrete values of these parameters in a two dimensional grid (a_m, τ_n) such that $a_m = a_o^m$ and $\tau_m = a_m\tau_n = a_m n\tau_o$ where a_o and τ_o are base values of the parameters and m and n are integers. A choice of an octave dilation factor with a_o=2, so that a_m=2^m and a dyadic translation so that τ_o=1 and τ_m = $2^m n$ gives an orthogonal set of wavelets for the Mexican Hat family and the transform then becomes:

$$W_{\psi,s}(m,n) = 2^{\frac{-m}{2}}\int_{-\infty}^{+\infty} s(t)\psi(2^{-m}t-n)dt \qquad (7)$$

In the case of a digitized signal $s(t_k)$ where $t_k = kT_s$ and $T_s = 1/f_s$, the sampling rate, represented as the sequence of N samples $s(k)$, k=0,1,2….N-1, the Discrete-Time Wavelet Transform is given as:

$$W_{\psi,s}(m,n) = 2^{\frac{-m}{2}}\sum_{k=0}^{N-1} s(k)\psi(2^{-m}k-n) \qquad (8)$$

where m=1,2,3,……log_2 N so that the number of octaves of scaling is limited to concur with the length of the sequence.

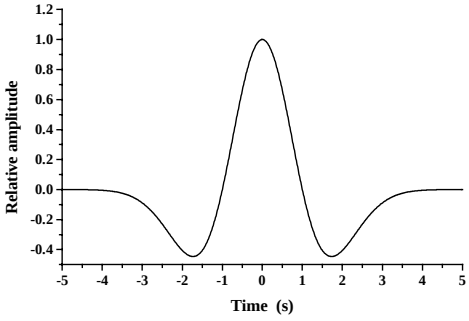

Fig. 2 The Mexican Hat Wavelet

Grossman *et al*. [4] showed that better identification of singular features in the signal could be obtained by the decomposition of each scale into several sub-scales or voices while maintaining octave scaling. This allows better frequency resolution to be obtained from a tight-framed set of wavelets. By choosing $a_o = 2^{1/M}$, where M is the number of voices per octave, the wavelet transform applied to a digitized signal $s(k)$ becomes:

$$W_{\psi,s}(m,n) = 2^{\frac{-m}{2M}} \sum_{k=0}^{N-1} s(k)\psi(2^{\frac{-m}{M}}k - n) \qquad (9)$$

When decomposed in this manner the time scales are referred to as levels where the level number is $2^{m/M}$.

2.2 Modulus Maxima

The total energy contained in the continuous wavelet transform at a scale factor a is given as:

$$E(a) = \int_{-\infty}^{+\infty} \left|W_{\psi,s}(a,\tau)\right|^2 d\tau \qquad (10)$$

This can be taken as a measure of the variance of the transform at scale factor a. The magnitude of the variance will reach its maximum value when the wavelet and the signal are coherent i.e. have similar frequency components present at similar positions in time. Locating maxima in the wavelet variance across scales therefore provides a means of determining the scales and translations at which the structure of the signal is coherent with the wavelet shape.

The value of the signal $s(t_o)$ at time $t = t_o$ influences the value of the wavelet transform within a domain of the form $|t - t_o| \le \sigma_\psi a$ where σ_ψ^2 is the variance of the analyzing wavelet function. This domain has a triangular shape in the time-scale plane, which converges to t_o as the scale factor a approaches zero and is known as the cone of influence.

The concept of modulus maxima was first introduced by Mallat [5,6]. A point $(a_o\ ,\ t_o)$ in the time-scale plane is referred to as a modulus maximum if:

$$\left|W_{\psi,s}(a_o,t_o)\right| > \left|W_{\psi,s}(a_o,t)\right| \text{ for } t < t_o \text{ and}$$
$$\left|W_{\psi,s}(a_o,t_o)\right| \ge \left|W_{\psi,s}(a_o,t)\right| \text{ for } t > t_o \qquad (11)$$

so that:
$$\frac{\partial}{\partial t}\left|W_{\psi,s}(a,\tau)\right|_{a_o,t_o} = 0 \qquad (12)$$

The modulus maxima can be thought of as points in the time-scale plane at which both the signal and the analyzing wavelet have local maxima. A line drawn across the scales which connects maxima belonging to the same point in the signal is called the modulus maxima line. Mallat & Hwang [5] have shown that a singular behavior in the signal $s(t)$ at time t_o means that there exists a modulus maxima line which converges towards the point t_o on the time axis as $a \to 0$. If there is no such line, then the signal is regular or smooth in the vicinity of $t = t_o$. Hence, modulus maxima lines in the time-scale plane may be used to identify singularities in the signal. Often the square modulus is used in place of its magnitude so that the modulus maxima are evaluated as:

$$\frac{\partial}{\partial \tau}\left[W_{\psi,s}(a,\tau)\right]^2_{a_o,\tau_o} = 0 \qquad (13)$$

The left-hand side of this expression can also be written as:

$$\frac{\partial}{\partial \tau}\left[W_{\psi,s}(a,\tau)\right]^2 = \frac{\partial}{\partial \tau}\left[W_{\psi,s}(a,\tau)\right].W^*_{\psi,s}(a,\tau) + \frac{\partial}{\partial \tau}\left[W^*_{\psi,s}(a,\tau)\right].W_{\psi,s}(a,\tau) \qquad (14)$$

where $W^*_{\psi,s}(a,\tau)$ is the complex conjugate of $W_{\psi,s}(a,\tau)$. For real valued signal and wavelet functions this becomes:

$$\frac{\partial}{\partial \tau}\left[W_{\psi,s}(a,\tau)\right]^2 = 2\left\{\frac{\partial}{\partial \tau}\left[W_{\psi,s}(a,\tau)\right].W_{\psi,s}(a,\tau)\right\} \qquad (15)$$

After appropriate substitutions for both functions on the right hand side of this expression and further simplification, it can be shown that:

$$\frac{\partial}{\partial \tau}\left[W_{\psi,s}(a,\tau)\right]^2 = 2a^3\dot{s}(\tau)\ddot{s}(\tau)\left[\int_{-\infty}^{+\infty} t.\psi(t)dt\right]^2 = 0 \qquad (16)$$

Since the third function on the right hand side of this equation is non-zero, the condition is satisfied when either $\dot{s}(\tau)$ or $\ddot{s}(\tau)$ is zero. Now $\dot{s}(\tau) = 0$ at maxima or minima in the signal while $\ddot{s}(\tau) = 0$ at points of inflexion. Hence the locations of the square modulus maxima of the wavelet transform can be used directly to identify the maxima, minima and points of inflexion in the signal being analyzed.

2.3. Wavelet Skeleton

A ridge vector for a given feature in the signal is formed when modulus maxima belonging to the same point in the signal are traced across increasing levels of analysis to the highest level used. Although the precise locations in time of the modulus maxima associated with a particular feature vary slightly across levels, they are always identified as the closest maxima points in time as the level increases [5,6]. Modulus maxima in the wavelet transform caused by noise occur sporadically, while those due to singularities in the signal are sustained across levels and this allows the two to be distinguished from each other. In addition modulus maxima due to signal features converge very definitively to a final position in time as the level is increased. A small amount of thresholding applied to the modulus maxima in generating the ridge vectors will eradicate those caused by noise at lower and middle levels of analysis so that only those caused by features of the signal will contribute to ridges. If chains are plotted on the time-scale plane connecting the points of individual ridges together for the entire signal a wavelet transform skeleton of the signal is obtained.

The skeleton of a single cardiac cycle of an ECG signal is shown in Fig. 3. At very low analysis levels where the wavelet spans the entire time scale, significant modulus maxima occur only at central points in the signal where most of its energy is concentrated. Consequently, the features of the

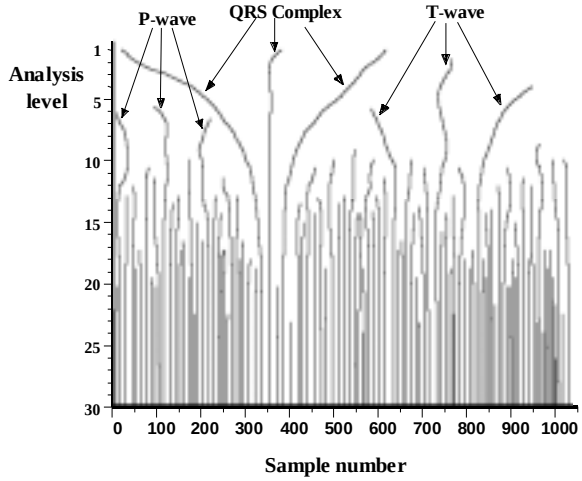

Fig. 3 The skeleton of the modulus maxima of a single cardiac cycle

QRS complex emerge first but the onset and termination of this component are not accurately located on the time scale. As the level is increased and the wavelet contracts, other prominent features of the signal occupying shorter periods of time generate modulus maxima above the threshold. It can be seen that the features of the P-wave and T-wave become established around level 7. At higher levels the locations of the onset, peak and termination points of these components approach their true values while other less pronounced features of the signal begin to generate ridges under the influence of the more compressed wavelet. Finally, at very high analysis levels even minor variations in the morphology of the signal caused by quantization and interference contribute to the skeleton, while the ridges of the components in the signal of interest have converged to their final values. By tracing the paths of the modulus maxima ridges established at lower analysis levels to their final convergence, the precise positions of the onset, peak and termination points for the QRS complex, the P-wave and the T-wave can be determined. It can be seen that these values have fully converged at level 22. From these positions on the time scale, the duration of these components can be calculated as well as the other segments and intervals of the signal defined in Fig. 1.

3. DATA ACQUISITION AND PREPROCESSING

Resting and exercise ECGs were recorded from 10 male and 11 female patients between 13 and 65 years referred to a hospital stress test unit. ECGs were recorded for a period of 3 minutes with the subject lying down resting. Following this, exercise ECGs were recorded for a period of 12 minutes with the subject on a treadmill, the speed and incline of which were slowly increased until the subject's heart-rate approached its maximum value (estimated as 220 - age(yrs) beats/min.). A recovery recording was then made following the exercise, with the subject lying down again until the heart rate returned to its resting value.

ECGs were monitored using a Marquette Mac-12 recorder, which provided an analogue lead-II output signal that was fed through a bandlimiting, anti-aliasing filter having a cut-off frequency of 200Hz to an analogue-to-digital converter card in a personal computer. Data was sampled at a rate of 1.64kHz with 12-bit resolution and stored on the hard disk. The digitized signals were then pre-processed by applying digital filtering algorithms in succession to the data. A low-pass filter having a cut-off frequency of 200Hz, a high-pass filter with a cut-off frequency of 0.5Hz and a notch filter centered around 50Hz were used to remove noise, baseline drift and mains interference respectively. This also helped to eliminate out-of-band movement artefact and muscle noise. Recordings were then scanned both automatically and manually to identify premature, ectopic and irregular beats as well as any other anomalies or artefact and offending recordings were discarded.

4. SIGNAL ANALYSIS

Data files of the ECG recordings were imported into MathLab (MathWorks Inc.) where all computations were carried out. Initially, long sequences of data were processed to obtain the wavelet transform of the entire recording of each subject up to level 12, i.e. 4 voices over the first 3 octaves of scaling and the modulus maxima were established in each case. Ridge vectors were traced up to level 12 to detect the peaks of the QRS complexes exclusively, which allowed successive cardiac cycles to be identified in the recordings. The corresponding heart rate to the nearest beat/min. was then determined for each cardiac cycle.

Following this, data files for individual subjects were segmented into lengths of 1024 samples suitably positioned around the QRS complex and were categorized according to heart rate with a 1beat/min. resolution over the full range, which extended from 46-184 beats/min. Sequences having the same heart rate were aligned so that the positions of their QRS complexes coincided in time.

Data sequences having the same heart rate were then processed in cross ensembles of 5 in a parallel 5-stage median filter, which removed any impulse-like interference present and also significantly reduced the quantization noise associated with the digitization process. The wavelet transform was then computed for each resulting sequence using 4 voices over 10 octaves of scaling and the modulus maxima were evaluated in each case. From this, skeletons of the transforms similar to that shown in Fig. 3 were constructed. Ridges in the skeleton were then traced for convergence to a fixed position in time, which was usually reached once the position of a ridge remained unchanged over 4 consecutive levels. Having already identified the position of the QRS complex, zones in the skeleton were searched on either side of this to determine the precise locations of the peaks of the P and T waves to within one sample time. Subsequently, the onset and termination of the QRS complexes and the associated P and T waves were determined with the same precision. This allowed the values of all of the components of the ECG signal defined in Fig. 1 to be established for each individual data sequence. This resulted in several values being obtained for each component, at each value of heart rate in the range covered.

5. VERIFICATION

The accuracy of the wavelet based method of identifying the timing of ECG components was verified by applying the technique to a test ECG signal. This test signal was obtained from the data file of a previously digitized ECG recording, which had been manually modified to remove noise and interference and to idealize the waveform structure. The file was stored in a Read Only Memory (ROM) and could be read out through a digital-to-analogue converter followed by a low-pass filter to generate an output signal simulating an ECG. From the addresses of samples in the data file the positions of the peak, onset and termination points of the waves were known exactly. The rate at which the contents of the ROM were read out allowed the effective heart rate of this test signal to be varied as desired.

This analogue signal was re-sampled, stored and processed in the same manner as the clinical recordings. The wavelet analysis method was applied to the test signal to

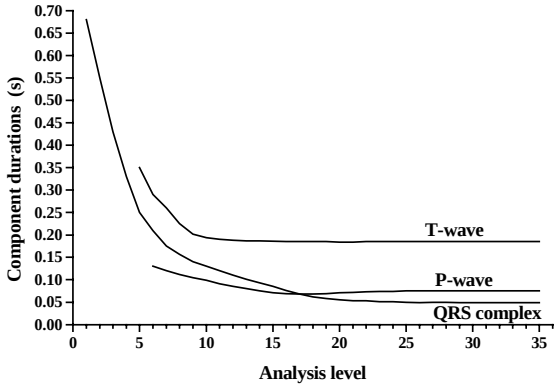

Fig. 4 The convergence of measured ECG components

determine the timing of its components at heart rates of 70, 80, 90, 110,120, 180 and 190 beats/min. The values obtained for all timing measurements made at all heart rates were within $\pm$1ms of the true values established from the data file with the exception of a single error of –3ms. The convergence of the values measured for a test signal at a heart rate of 70 beats/min., having a P-wave duration of 75ms, a T-wave duration of 186ms and a QRS complex of 50ms is shown in Fig. 4.

6. RESULTS

The data obtained from the subjects above were processed to obtain a characteristic equation for each component of the ECG signal which would describe the variation in its duration as the cardiac cycle time altered inversely with heart rate. The values of each component measured at the same heart rate were averaged to give a single value for each component. Averages were obtained as a function of the cardiac cycle time for male and female subjects separately and for all of the subjects combined. Second order equations in the square root of the cardiac cycle time of the form $A\sqrt{T_{R\text{-}R}} + BT_{R\text{-}R} + C$ were then fitted to the data for each component of the ECG using a least-mean-square error method. The data obtained from the combined male and female subjects for each of the constituent components are

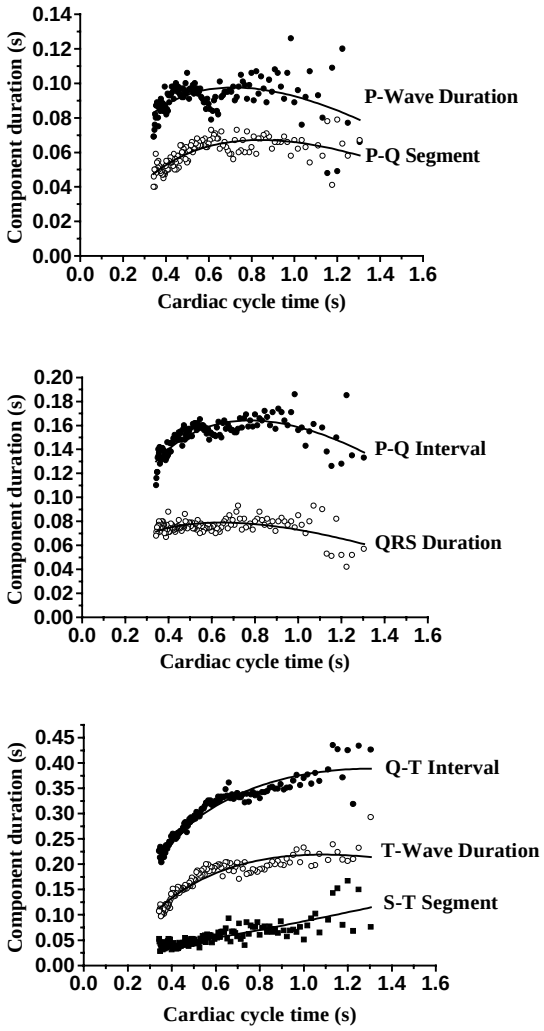

Fig. 5 Data obtained from combined subjects with 2nd-order curves fitted

shown plotted in Fig. 5. As data points were obtained with a 1beat/min resolution in heart rate, they are closely spaced and standard deviation bars have been omitted for clarity but ranged typically from 3 - 15ms. The corresponding equations fitted are:

$$T_{P-Wave} = 0.37\sqrt{T_{R-R}} - 0.22T_{R-R} - 0.06 \quad s \tag{17}$$

$$T_{P-Q\,Seg} = 0.33\sqrt{T_{R-R}} - 0.18T_{R-R} - 0.08 \quad s \tag{18}$$

$$T_{P-Q\,Int} = 0.69\sqrt{T_{R-R}} - 0.39T_{R-R} - 0.14 \quad s \tag{19}$$

$$T_{QRS} = 0.25\sqrt{T_{R-R}} - 0.16T_{R-R} - 0.02 \quad s \tag{20}$$

$$T_{Q-T\,Int} = 1.21\sqrt{T_{R-R}} - 0.53T_{R-R} - 0.31 \quad s \tag{21}$$

$$T_{T-Wave} = 1.06\sqrt{T_{R-R}} - 0.51T_{R-R} - 0.33 \quad s \tag{22}$$

$$T_{S-T\,Seg} = -0.09\sqrt{T_{R-R}} + 0.13T_{R-R} + 0.04 \quad s \tag{23}$$

While coefficients in the equations obtained were somewhat different for male and female subjects the trend was the same for all components and the range of values was not greatly different. Values for female subjects were a little lower and showed a slightly lower dependence on heart rate.

7. CONCLUSION

Fig. 6 shows a lead-II ECG signal, which has been synthesized from this set of equations at a heart rate of 140 bpm. Stored files were used to generate the profiles of the P and T waves. Changes in the timing of the constituent components are an accurate reproduction of those observed *in vivo*. It is the intention of the authors to use these equations as the foundation for a versatile micro-controller based ECG simulator, which will provide an output signal having user adjustable properties and a profile which behaves in a manner closely aligned to that of the *in-vivo* ECG.

REFERENCES

[1] H. C. Bazett, "An analysis of the time relations of the electrocardiogram," *Heart*, vol. 7, pp. 353-370, 1920.

[2] W. Adams, "Normal duration of the electrocardiographic ventricular complex," *J. Clin. Invest.*, vol. 15, p. 335, 1936.

[3] J. Sandor and S. Louis, "The duration of the Q-T interval as a function of heart rate," *Amer. Heart J.*, vol. 110, pp. 872-876, 1985.

[4] A. Grossmann and J. Morlet, "Decomposition of the Hardy function into square integrable wavelets of constant shape," *Siam J. Math. Anal.*, vol. 15, pp. 723-736, 1984.

[5] S. G. Mallat and W. L. Hwang, "Singularity detection and processing with wavelets," *IEEE Trans. Infor. Theory*, vol. 38, pp. 617-643, 1992.

[6] S. G. Mallat and S. Zhong, "Characterization of signals from multiscale edges," *IEEE Trans. Pattern Anal. & Machine Intell.*, vol. 14, pp. 710-732, 1992.

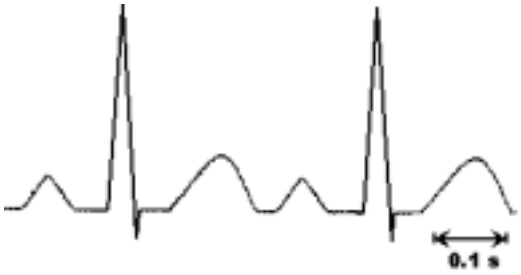

Fig. 6 Waveform of a simulated ECG signal at 140 bpm